RSC Advances

ROYAL SOCIETY OF CHEMISTRY

www.rsc.org/advances

Metal ion binding properties of a bimodal triazolyl-functionalized calix[4]arene on a multi-array microcantilever system. Synthesis, fluorescence and DFT computation studies

Abdullah N. Alodhayb,[a] Mona Braim,[a] L.Y. Beaulieu[a], Gopikishore Valluru,[b] Shofiur Rahman,[b] Ahmed K. Oraby[b] and Paris E. Georghiou[b*]

Abstract: A bimodal calix[4]arene functionalized with triazolyl-linked anththracenyl and 3-propylthio-acetate groups is described. This new calix[4]arene formed an effective SAM on Au in a multi-arrayed microcantilever instrument and was shown to be a sensitive receptor to low concentrations of Hg^{2+}. Competitive studies confirmed the Hg^{2+} sensitivity. DFT computational studies were in agreement with the likely site of binding of the metals.

1 Introduction

We have previously reported on our studies involving the functionalization of both the upper- and lower-rims of calix[4]arene in attempts to modify the gold surfaces of microcantilevers.[1a-c] This work was directed at producing aqueous metal-ion specific or selective sensors for the ultimate aim for the development of a real-time environmental effluent water monitor.

Calix[4]arene, its homologues and derivatives have been extensively studied and their chemistry and applications have been widely reported.[2a-c] The main features which make calixarenes widely applicable are the fact that in particular for calix[4]arene, besides having a relatively robust core macrocyclic structure, it can be selectively functionizated[3a,b] at either or both of its rims (Figure 1). We[1a-c] (and many others[4]) have shown that with appropriate functional groups, a calix[4]arene can both bind with a gold surface to form a stable self-assembled monolayer (SAM) and also carry a ionophoric functional group which can selectively bind to specific metal cations.

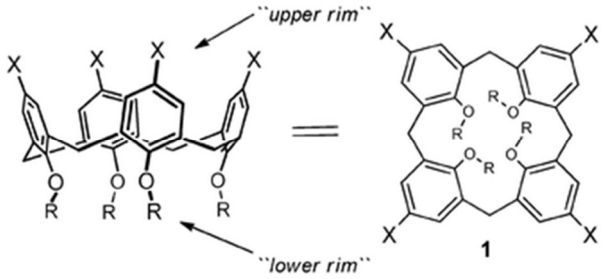

Fig. 1. A schematic representation of the general structure of calixarenes where X and R respectively represent the possible upper and lower rim functional groups.

Besides being employed in atomic force microscopy (AFM) for surface imaging, microcantilevers have been actively used as sensors for the detection of various physical, biological and chemical phenomena.[5-7] Detection changes in temperature, DNA hybridization and metal ions in aqueous solution are some examples of the possible applications of microcantilever (MCL) sensors.[8,9] The attractive characteristics of MCL sensors, such as high sensitivity and selectivity, label-free and real time detection, cost-efficiency, fast response time, etc. have also extended the application of MCLs to include medical and pharmaceutical applications.[10,11] The operation of these sensors depends on choosing an appropriate receptor which is immobilized on one side of the MCL. When the target analyte of interest interacts with the receptive or "sensing" layer, a surface stress develops leading to the mechanical deflection of the MCL. Such deflections can be monitored using several approaches, such as for example, the optical beam deflection system.[12] Since microcantilever sensors are also sensitive to environmental effects such as change in temperature and pH, the use of a reference MCL is necessary to subtract any parasitic deflection caused by these effects. Therefore, most MCL sensor results reported in the literature are conducted using two MCLs, one acting as the active and the other as a reference.

In addition to using reference cantilevers, cantilever sensor experiments are often repeated several times in order to assure the reproducibility of the results. Although repeating the sensing experiments may examine the reproducibility, ensuring the existence of comparable experimental conditions is not often trivial or possible. Using two single cantilevers at the time is also very time-consuming. Therefore, the work reported in this paper was conducted using two MCL sensor arrays each consisting of eight identical cantilevers. Such MCL arrays offer a great advantage in being able to ensure identical conditions for all of the active and reference MCLs.

In this paper, we report on the data collected using a 16-microcantilever array system for the detection of heavy metals in aqueous solution. The gold-surfaces of the MCLs are functionalized with SAMs produced from a bimodal *cone*-calix[4]arene **2** (Scheme 1) whose *distal*– or, *1,3*–positions, on the lower-rim are functionalized with 9-methylanthracenyl moieties linked via triazolyl groups to the calix[4]arene lower rim. Each of the upper rim positions are functionalized with a 3-propylthioacetate [$-(CH_2)_3SAc$] group. As illustrated in Fig. 2, the Au-coated microcantilvers are chemically modified by the formation of SAMs of the calixarene sensing layer. Analyte cations, such as Hg^{2+}, could then preferentially bind with the receptor molecules in the triazolyl region as shown in Fig, 2. Binding events such as these cause bending of the MCL produced by the surface stress. The strength and selectivity of the binding events are demonstrated by the magnitude of the MCL deflection.

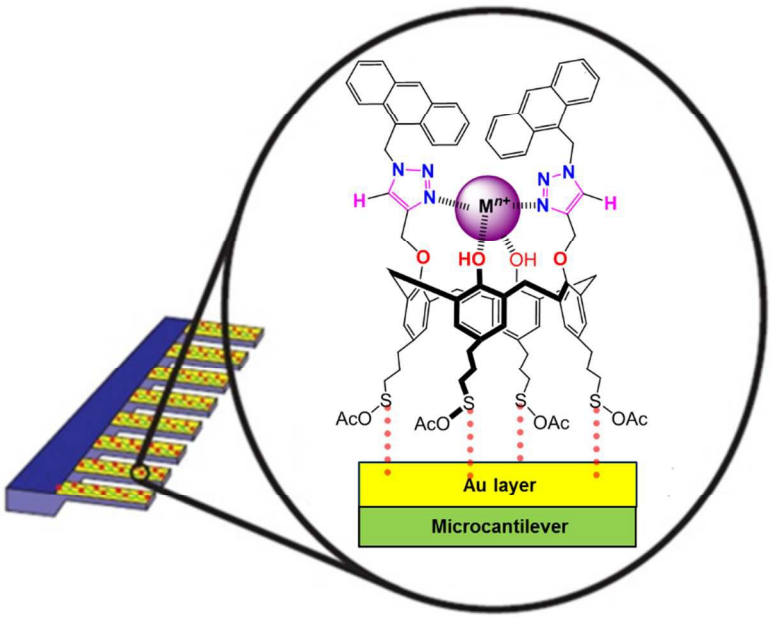

Fig. 2: A schematic representation of a microcantilever array consisting of 8 cantilevers. Each cantilever can be individually functionalized. *Inset:* the chemical structure of calix[4]arene **2** along with the site of the binding of the target cation (Hg^{2+}).

Detecting the presence of heavy metal contamination (e.g. Pb^{2+}, Cd^{2+}, Ni^{2+}, Zn^{2+}, Hg^{2+}, Cu^{2+}, Fe^{3+}) in freshwater lakes etc, is of paramount importance for both humans and the environment. The hazardous effects of heavy metals are not only observed when they are in high concentrations, but also trace concentrations could have significant toxic effects.[13] Therefore, environmental considerations require that these metal ions be monitored in order to prevent the possible contamination of both humans and fish habitats. A real-time monitoring device for such toxic metals is arguably highly desirable.

2. Results and discussion

Calixarenes which incorporate stable and functional 1,2,3-triazolyl units that have been used as binding sites for cations, especially transition metal ions, have previously been reported by others,[14,15a-e] and an analogous system was chosen for the particular work described herein. The functionalization of the calixarenes with triazolyl groups is

achieved through the use of a "click", or as it is more precisely known, a Cu(I)-catalyzed azide-alkyne cycloaddition ("CuAAC") reaction.

In our work reported herein, the synthesis of the upper- and lower-rim bimodal calix[4]arene derivative **2** was targeted for its potential use *both* as a sensing layer on gold-coated MCLs and also for selective binding of various metal ions which could potentially be correlated by fluorescence titrations in solution studies which were conducted simultaneously and which are described first below.

2.1 Synthesis of the bimodal calix[4]arene 2

The anthracenyl-triazolyl functionalized bimodal calix[4]arene **2** which was used as the sensing layer in this study was synthesized in an analogous manner to those described by others,[14,15a-d] as outlined in Scheme 1, using, however, as one of the synthetic precursors, 5,11,17,23-tetrakis(3-propylthioacetate)calix[4]arene (**3)** which we have previously reported.[1a-c] Alkylation of **3** with propargyl bromide afforded the 1,3-di-*O*-propragylated calix[4]arene **4** in 71% yields.

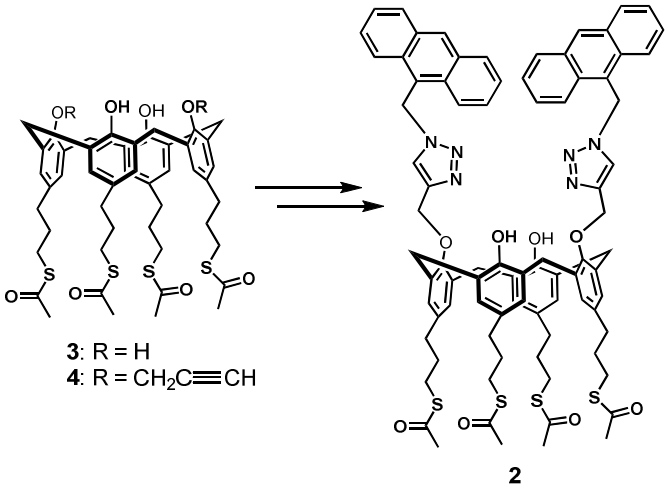

Scheme 1. Synthesis of bimodal calix[4]arene **2** .

The reaction of **4** with 9-(azido-methyl)anthracene[15a,e] under "click" (or CuAAC) reaction conditions with CuI catalysis[15] in a THF/H_2O mixed solvent system at 60 °C for 24 h afforded **2** as a pale yellow solid in 69% yield. It was characterized by ^{1}H- and ^{13}C-NMR spectroscopy and mass spectrometry. The formation of the 1,2,3-triazole rings in **2** was apparent from the appearance of the triazole-*H* signal as a two-proton singlet at δ 7.23 ppm. A second four-proton singlet signal due to the anthracene-CH_2-triazole methylene protons was affected by the triazole unit and was observed at δ 6.40 ppm and its corresponding C-13 chemical shift was present at δ 46.4 ppm. The signal at δ 4.75 ppm corresponding to the –OCH_2-triazole linkers also appeared as a four-proton singlet and its corresponding C-13 chemical shift at δ 69.2 ppm. The ^{1}H-NMR spectrum suggested that the calix[4]arene unit is in a *cone* conformation since the proton chemical shifts of the bridging –CH_2– groups appeared as a pair of four-proton AB doublets at δ 3.59 ppm and 2.77 ppm (J = 13.1 Hz). The corresponding ^{13}C chemical shift was observed at δ 34.0 ppm. There are eight aromatic protons (Ar-*H*), four of which appear as singlets at δ 6.34 and 6.57 ppm. A two-proton singlet at δ 6.83 ppm is due to the hydroxyl groups. A singlet at δ 8.39 ppm, two doublets at δ 8.18 ppm and 7.96 ppm and a multiplet centred at δ 7.45 ppm correspond to the anthracene moiety. Four triplets at δ 2.86, 2.60, 2.51 and 2.16 ppm and two multiplets at δ 1.84 and 1.50 ppm, correspond to the propyl chains liking the thioacetate groups which appear as two six-proton singlets at δ 2.30 and 2.35 ppm, whose corresponding ^{13}C chemical shifts are observed at δ 195.8 and 195.9 ppm. APCI-LC/MSD also confirmed the expected mass of **2** and clearly showed a m/z signal at 1431.6 $[M+1]^+$ and also confirmed by HRMS.

2.2 Fluorescence complexation studies

Association constants (K_{assoc}) based on the fluorescence data obtained were calculated using Thordarson's global-fit method.[16a,b] The complete spectra recorded from each of the fluorescence titrations can be analyzed in this way, instead of relying on selecting the changes of specific selected wavelengths. Calixarene **2** displayed monomer emission in the 360-565 nm range and at the 350 nm excitation wavelength. The fluorescence emissions were quenched (apart from Zn^{2+} and Cd^{2+} which showed enhancement- *see below*) upon adding the metal ions as a result of complexation occurring between **2** and the individual guest metal ions. The cations that were investigated were Ag^{+}, Co^{2+}, Cd^{2+}, Fe^{2+}, Fe^{3+}, Cu^{2+}, Hg^{2+}, Pb^{2+}, Zn^{2+}, Ni^{2+} and Mn^{2+}, all of which were used as their respective perchlorate salts. Fluorescence spectroscopic titration studies showed that **2** is highly sensitive to Hg^{2+} and Fe^{3+}, and to a lesser extent Pb^{2+}. Fig. 3 shows for example, the fluorescence titration experiments conducted for **2** with $Hg(ClO_4)_2$. The fluorescence intensities of **2** gradually decreased as the concentration of Hg^{2+} ions increased from 0.18 to 6.8 molar equivalents. The fluorescence quenching of **2** may be explained by either a photoinduced electron transfer (PET) or by a heavy-atom effect.[17a-c] In the former case, when the Hg^{2+} ion is bound by the two triazole nitrogen atoms, the anthracene units may behave as PET donors whereas the triazole unit behave as electron acceptors. The resulting global K_{assoc} was determined to be 1.33×10^5 M^{-1} with a covariance of fit value of < 0.01 which is a reasonably good fit of the data to the model. The RMS value is also good as can be seen in the Residual/SE plot[16a,b] shown in the SI.

With respect to the apparent quenching of the fluorescence upon the addition of $Fe(ClO_4)_3$ a calculated *apparent* K_{assoc} of 1.17×10^5 M^{-1} could be determined. However, whilst this value appeared to be of a similar magnitude to that measured with Hg^{2+}, in a

related project, we became aware of an excellent study on the behaviour of $Fe(ClO_4)_3$ with a related calixarene ionic receptor which was published during the same time that the present work was being completed. W.-S. Chung and coworkers[18] demonstrated that $Fe^{3+}$was capable of oxidizing both the appended anthracenyl groups and *also* one or both of the free-phenolic groups in their particular calixarene system. It is therefore highly likely on the basis of Chung's work, that for the case with $Fe(ClO_4)_3$, that a similar occurrence could be involved with our system both in the aqueous MCL system and in the fluorescence study. In our case, the anthracenyl groups could similarly be undergoing oxidation reactions.

Table 1 and Fig. 4 summarizes the K_{assoc} values determined for all of the metal complexes studied, with those for Hg^{2+} , Fe^{3+} and Pb^{2+} being the largest, in the order shown, but only by factors of 1.1 to 3.0 in going from Hg^{2+} to Fe^{3+} and from Hg^{2+} to Pb^{2+}

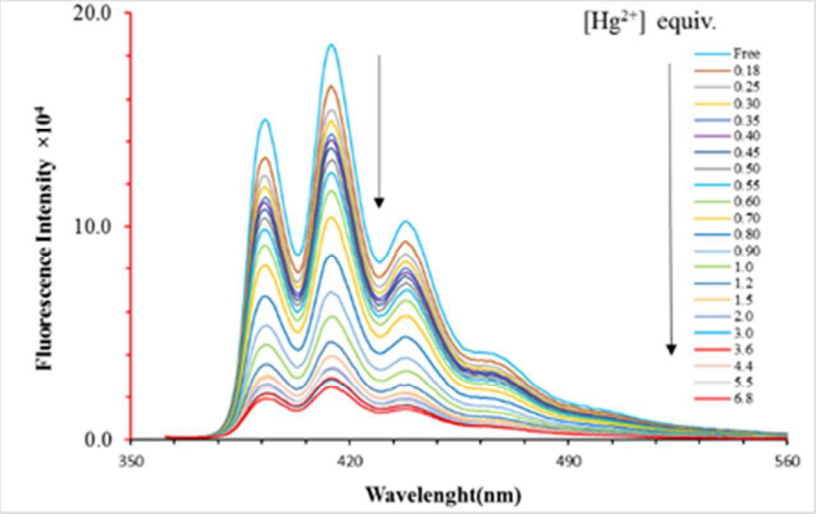

Fig. 3. Fluorescence spectra of **2** upon addition of Hg^{2+} (0.18-6.8 eq) in acetonitrile/chloroform (v/v= 9:1) solutions. λ_{ex} = 350 nm.

Table 1. K_{assoc} values of complexes of **2** with metal perchlorates.

Entry	M^{n+}	M^{n+} mol equiv.	$K_{assoc} \times 10^3$ M^{-1} [cov(fit)]
1	Hg^{2+}	0.20-6.8	133 [0.0040]
2	Fe^{3+}	0.20-11	117 [0.0014]
3	Pb^{2+}	0.30-16	45.3 [0.0081]
4	Cd^{2+}	1.1-15	14.0 [0.00097]
5	Co^{2+}	1.7-8.2	8.29 [0.0091]
6	Zn^{2+}	0.90-36	6.85 [0.0012]
7	Cu^{2+}	1.1-36	3.95 [0.017]
8	Fe^{2+}	0.80-68	3.18 [0.0098]
9	Ni^{2+}	0.38-60	1.30 [0.0015]

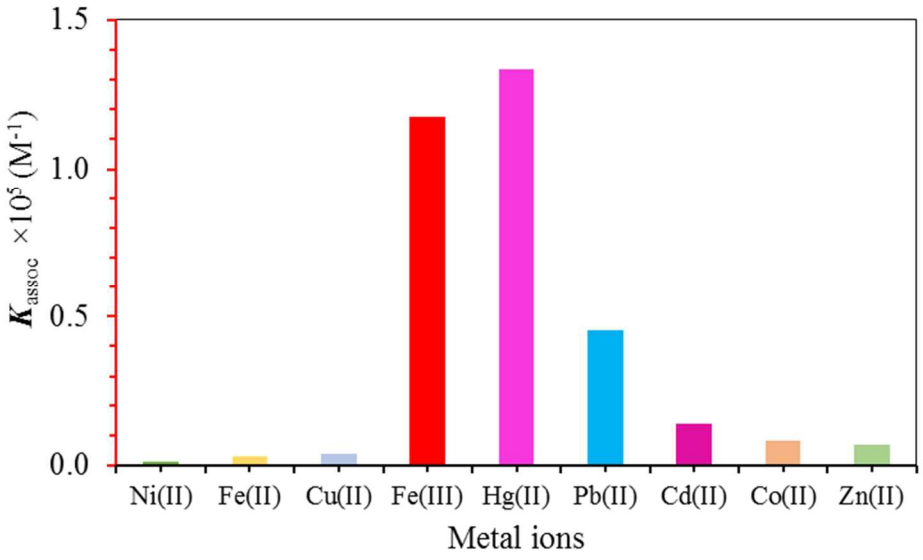

Fig. 4. Histogram showing the K_{assoc} values calculated by using the global fit analysis of the fluorescence titrations of **2** with different metal ions.

2.3 Metal competitive experiments

To evaluate further any potential selectivity of **2** towards Hg^{2+} over the other metal ions examined, competitive experiments were carried out with different metal ions. In these

experiments, stock solutions of **2** (2.0×10^{-5} M) and each of the metal perchlorate salts (1.5×10^{-2} M) were prepared in a 9:1 CH_3CN:$CHCl_3$ solvent. To each solution which contained equimolar amounts of each of the respective metal ions (M^{n+}) with **2**, a molar equivalent of $Hg(ClO_4)_2$ was added. The fluorescence emissions of the resulting solutions were quenched (Fig. 5).

It is noteworthy that whereas with the exception of Zn^{2+} or Cd^{2+}, all of the metal ions tested with **2**, exhibited fluorescence quenching, With Zn^{2+} or Cd^{2+}, the fluorescence emissions were slightly enhanced (Fig. 6). In both of these cases however, when equimolar amounts of Hg^{2+} were added, fluorescence quenching occurred. Similar chelation fluorescence enhancement with Zn^{2+} and Cd^{2+} has been reported by others.[19]

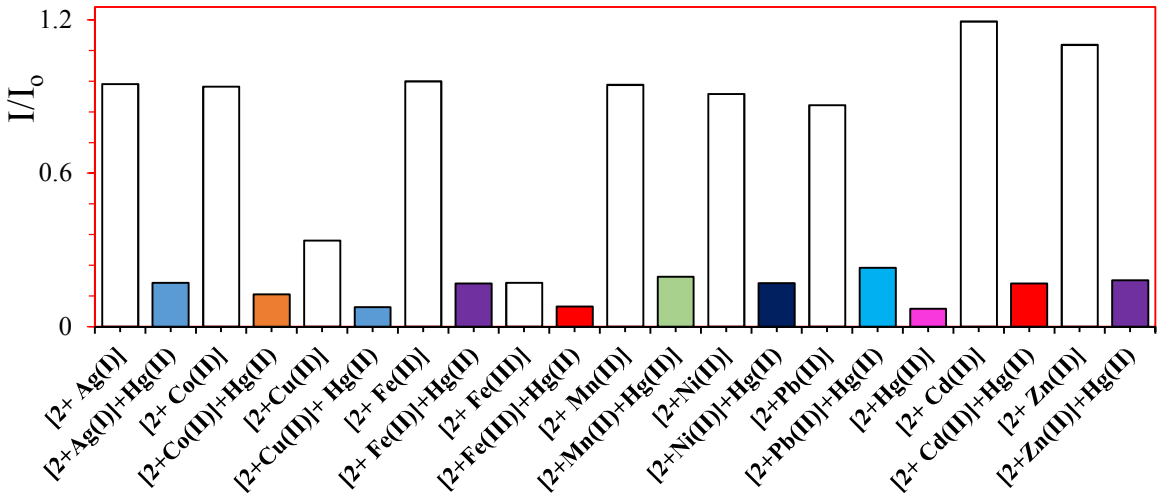

Fig. 5. Histogram showing the different degrees of fluorescence quenching for the solutions of 1:1 **2**:M^{n+} to which equimolar amounts of Hg^{2+} were added

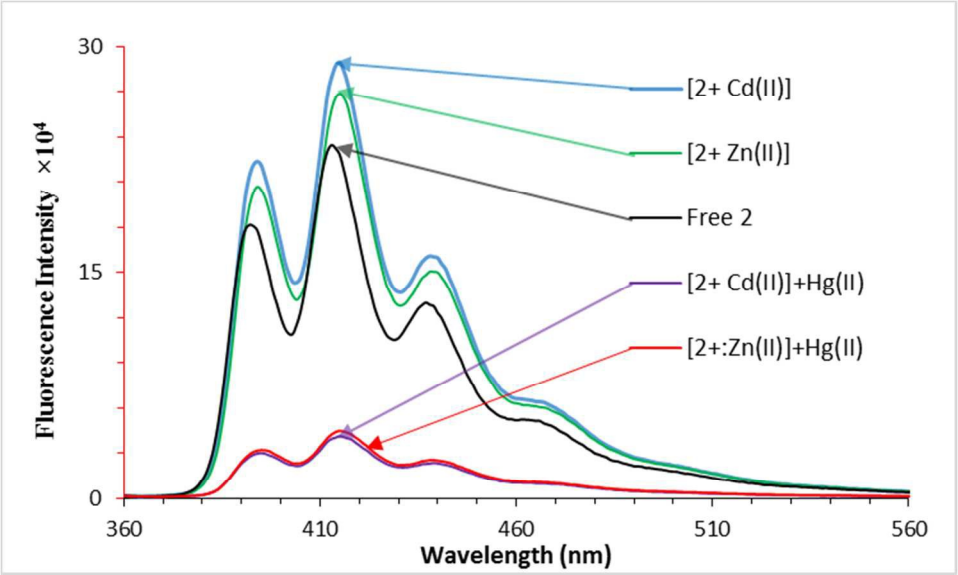

Fig. 6. Fluorescence emission enhancement shown when equimolar amounts of $Cd(ClO_4)_2$ and $Zn(ClO_4)_2$ were added to the 1:1 solutions of solutions of 1:1 **2**:M^{n+}

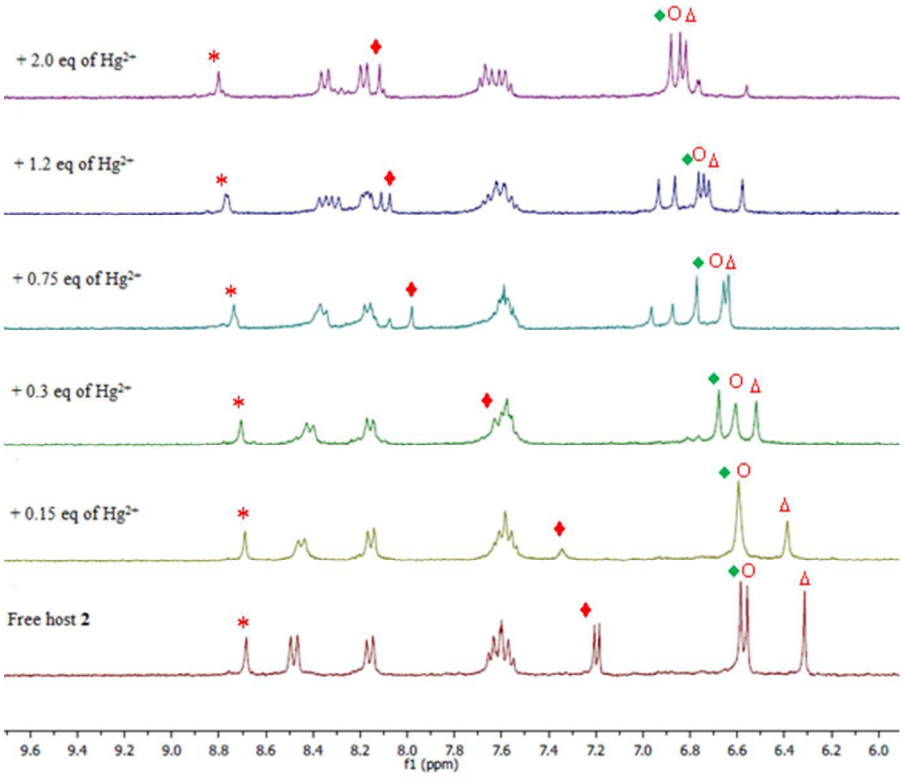

Fig. 7. Partial ^{1}H-NMR (300 MHz) spectra at 298K for the titration of **2** with $Hg(ClO_4)_2$ in 4:1 (*v/v*) CD_2Cl_2:CD_3CN; ✱,♦, **o**, **Δ**, and ♦ denote the changes for the anthracene-*H* (δ 8.68–8.80 ppm), triazolyl-*H* (δ 7.20–8.11 ppm), triazolyl-C*H*$_2$-anthracene (δ 6.56–6.84 ppm), and Ar-*H* (δ 4.91–5.03 ppm) protons, respectively.

2.4 Complexation studies of 2 with Hg^{2+} using ^{1}H-NMR spectroscopy

To shed further insight into the mode of the complex formation between **2** and Hg^{2+} observed by the fluorescence titrations, a ^{1}H-NMR titration experiment was conducted. Addition of aliquots of $Hg(ClO_4)_2$ to a solution of **2** in the same 4:1 CD_3CN:CD_2Cl_2 (*v/v*) solvent system, resulted in the downfield chemical shifts shown in Fig. 7. No significant other changes were observed for the remaining regions of the spectra, suggesting that the Hg^{2+} interacts in the region of the calix[4]arene **2** lower rim and the anthracenyl moiety, within the "N-O-O-N" core formed by the two *distal* calixarene hydroxyl groups and one nitrogen atom of each of the triazolyl groups) as depicted in Fig.2. This would likely explain the largest chemical shift change ($\Delta\delta$ = +0.91 ppm) which is observed from δ 7.20 to 8.11 ppm. This prediction is supported by the computation study conducted as described in the following section.

In order to determine whether under the solvent conditions used for the fluorescence measurements, $Hg(ClO_4)_2$ could oxidize **2** in an analogous manner to the observations made by Chung's group with the reactions of their receptors with $Fe(ClO_4)_3$,[18] we subjected 1,3-di-propoxycalix[4]arene (**1**: R = H; R_1= Pr; X = *t*-Butyl) to a titration experiment with up to 2-fold excess of $Hg(ClO_4)_2$ and $Fe(ClO_4)_3$. Even after 48 h no changes in the chemical shifts of any of the protons could be detected. Clearly, the presence of the anthryl-oxadiazole functional groups on Chung's calixarene scaffold has a strong activating effect towards its oxidation with the $Fe(ClO_4)_3$

Since our receptor is quite similar to that reported by Rao and coworkers,[14] a titration experiment was also conducted with $Co(ClO_4)_2$. In their case, their fluorescence titration experiments were conducted in ethanol (ours were in acetonitrile/chloroform, v/v= 9:1)

and their NMR experiments in DMSO-d_6. With our receptor molecule, titration with $Co(ClO_4)_2$ in DMSO-*d6* showed a similar up-field shift for the $–CH_2$-triazole- methylene bridge protons as in Rao's paper, but interestingly with **2** in the CD_2Cl_2:CD_3CN solvent system with $Hg(ClO_4)_2$ the chemical shifts observed are all down-field.

2.4 Mass spectrometric study

A mass spectrometric study was conducted with each of the three metal (i.e. Hg^{2+}, Pb^{2+}, and Fe^{3+}) perchlorates which showed the highest binding constants from the fluorescence titrations. Mixtures (1:1) of the perchlorates with **2** were prepared in the 9:1 CH_3CN:$CHCl_3$ solvent mixture used for the fluorescence titrations. Several mass spectrometric methods were examined, including APPI and ESI but MALDI-TOF afforded the most informative data. In the case of $Pb(ClO_4)_2$, experiments using MALDI-TOF and either anthracene, dithranol or α-cyano-4-hydroxycinnamic acid (CHCA) as matrixes, all gave a major ion at *m/z* = 1637.3 which corresponds to $[C_{84}H_{81}N_6O_8PbS_4]^+$ and is assigned to a complex formed between **2** and a single Pb^{2+} *i.e,* $[\mathbf{2}+(Pb^{2+} - 2H^+) + H]^+$. The isotopic pattern of signals for this ion exactly matched the theoretical predicted one (**Fig. SI 18**). MS/MS data of this signal revealed several daughter ions, in particular **at**, *m/z* = 1365.4 *i.e,* $[1637.2 - (C_{18}H_{14}N_3) + H^+]^+$ and *m/z* = 191.1 ***i.e*** $[C_{15}H_{11}^{\bullet}]^+$ which corresponds to the methylanthracenyl moiety. Other ions formed with the dithranol matrix, included *m/z* = 1495.2 *i.e* $[2 + Na^+ + CH_3CN]^+$ and 1453.3 *i.e* $[\mathbf{2} + Na^+]^+$, and corresponding daughter ions. The corresponding MALDI experiments of **2** with $Hg(ClO_4)_2$ did not yield a mass corresponding to $[\mathbf{2}+(Hg^{2+} - 2H^+) + H]^+$ or other corresponding ions that were seen with $Pb(ClO_4)_2$. In the case of $Hg(ClO_4)_2$ with dithranol as the matrix, *m/z* = 506/507 and 476/477 ions however were observed which correspond to $[C_{84}H_{80}Hg_3N_6O_8S_4]^{4+}$ and $[C_{86}H_{89}Hg_2N_7O_{10}S_4]^{4+}$ respectively which could tentatively be assigned to $[\mathbf{2} + (Hg^{2+} - 2H^+) + 2Hg^{2+}]^{4+}$ and $[\mathbf{2} + (Hg^{2+} - 2H^+) + Hg^{2+} + 2H^+ + 4H_2O)]^{4+}$ ions, respectively (**Fig SI 19**). The MALDI-TOF experiments with $Fe(ClO_4)_3$ afforded a major ion at *m/z* = 783 which corresponds to $[C_{86}H_{85}FeN_7NaO_9S_4]^{2+}$ and could tentatively be assigned to $[\mathbf{2} + (Fe^{3+} - 2H^+) + Na^+ + H_2O + CH_3CN]^{2+}$. MS/MS of this ion

gave daughter ions at *m/z* = 22.99 i.e. Na+ and at *m/z* = 559 which corresponds to $[C_{54}H_{58}FeN_6O_9S_4]^{2+}$ *i.e.* to [783 – {Na^+, CH_3CN, $(C_{15}H_{11})_2$}] involving a loss of both of the anthracenyl group (**Fig. SI 20**). The MALDI-TOF spectrum of **2** with itself dithranol matrix revealed a major signal at *m/z* = 1453.3 (**Fig. SI 16**) which corresponds to $[C_{84}H_{82}N_6NaO_8S_4]^+$ i.e. [**2** + Na] (**Fig SI 17**).

These results suggest that Hg^{2+} ions in particular, as compared to the Pb^{2+} and Fe^{3+}, can and do bind to more than a single site, in solution, most likely at the sulfur atoms of the thoacetate groups, in addition to the triazolyl moieties.

2.5 Detection of Hg^{2+} using triazolylcalixarene- functionalized microcantilever sensor arrays

Preliminary experiments were first conducted to determine the sensitivity of calixarene-functionalized MCLs towards specific heavy metals ions. An aqueous 2×10^{-5} M solution of $Hg(ClO_4)_2$ was introduced into the fluid cell which contained an array of both active and reference microcantilevers. As shown in Fig. 8, the triazole-functionalized MCLs underwent mechanical deflections, which can be attributed to the formation of surface stress due to the interaction between the calixarene receptor (sensor layer) and Hg^{2+} ions. The decanethiol-functionalized reference MCLs on the other hand, experienced much smaller deflections. The deflections shown by both the active and reference MCLs were very close, indicating the excellent reproducibility of these MCL arrays. The deflection of the reference MCLs, although small compared to the active ones, is likely due to the interaction between Hg^{2+} ions and areas of exposed Au atoms in regions where the SAM is incomplete, which is regularly observed with decanethiol SAMs.[20] Similar results indicating the Hg^{2+} adsorption on Au-coated MCLs were also reported by Xu et al.[21] who proposed that the bending of Au-coated MCLs exposed to Hg^{2+} ions was a result of the formation of Hg/Au amalgam on the Au surfaces. In order to exclude the deflections

resulting from any adsorption of Hg^{2+} ions on the Au surface, the measurements of the reference MCLs were subtracted from those of the active MCLs to produce the differential signals. The resulting signals, which are shown in Fig. 9, illustrate the MCL deflections caused by the specific binding between the calixarene sensing layers and the Hg^{2+} ions.

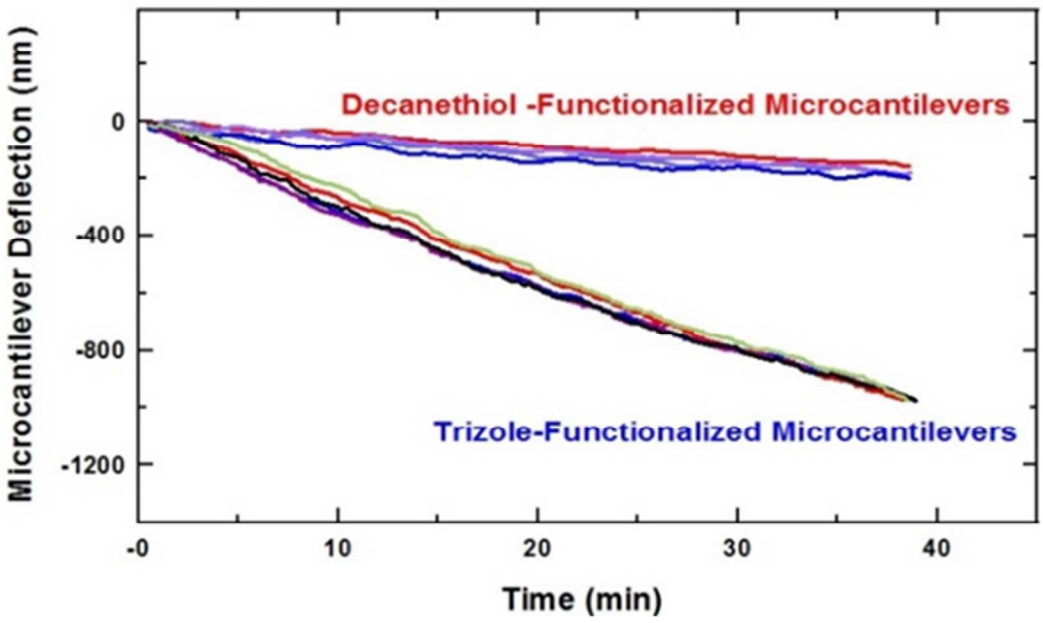

Fig. 8. Microcantilever deflection measurements of the eight functionalized microcantilevers obtained after the injection of a 2.0×10^{-5} M aqueous solution of $Hg(ClO_4)_2$

For the different concentrations of Hg^{2+} tested, Fig. 9 also shows that the calixarene-functionalized microcantilevers are capable of detecting interactions between calixarenes and Hg^{2+} for concentrations as low as 2×10^{-11} M. Increasing the target concentration implies that a larger number of target ions are interacting with the calixarene molecules immobilized on the microcantilever surface. This, in turn, causes an increase in the

microcantilever deflection. The microcantilever deflections obtained with a 2×10^{-11} M solution of the mercury salt was in the range of 180 nm to 200 nm, which is significantly larger than the signal noise, allowing, in principle, for smaller concentrations of Hg^{2+} to be detected. These results clearly reveal the high sensitivity of triazole-functionalized microcantilevers by responding differently to the injection of different concentrations of Hg^{2+}.

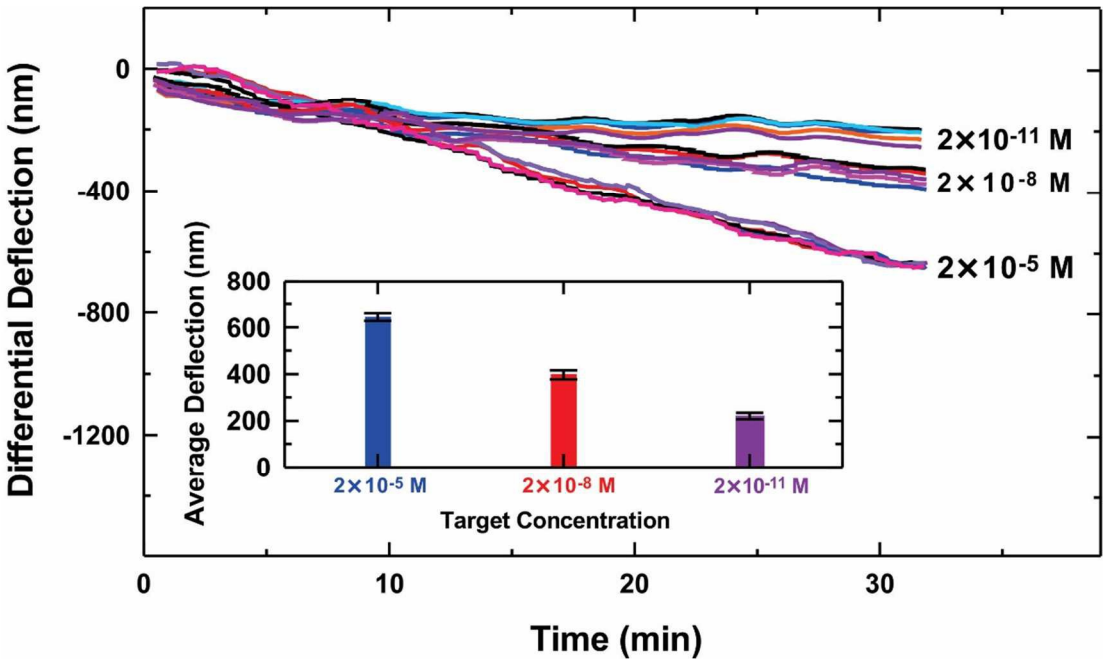

Fig. 9. Differential microcantilever deflections for three different concentrations of $Hg(ClO_4)_2$. Each curve represents the differential measurement (active signal–reference signal) of the microcantilevers in the array. The inset shows the average microcantilever deflection obtained from the three concentrations of $Hg(ClO_4)_2$. Each error bar represents the standard deviation obtained from each four microcantilevers exposed to the same concentration.

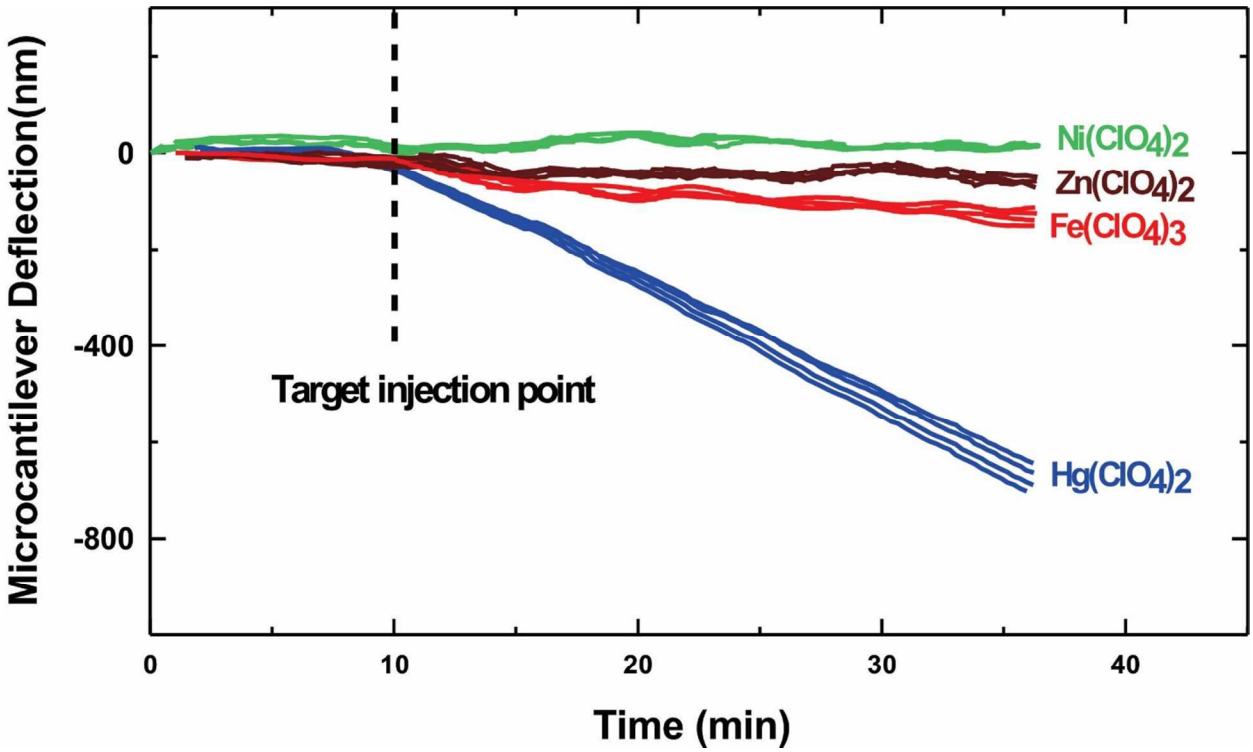

Fig. 10. Microcantilever deflection to 2×10^{-5} M aqueous solutions of $Hg(ClO_4)_2$ (blue), $Fe(ClO_4)_3$ (red), $Zn(ClO_4)_2$ (brown), and $Ni(ClO_4)_2$ (green).

Experiments were also undertaken to investigate the sensitivity of the triazole-functionalized MCLs in the presence of other metals ion in the solution. In particular, we were interested to see if the high sensitivity of triazole-functionalized MCLs towards Hg^{2+} ions would be altered in the presence of Pb^{2+} ions. In the first experiment, conducted with the same number of active and reference cantilevers as the experiments discussed above, a 2.0 10^{-5} M aqueous solution of $Pb(ClO_4)_2$ was first introduced into the cell containing triazole-functionalized MCLs for approximately 27 mins, followed by the injection of the same concentration of $Hg(ClO_4)_2$ for the same period of time. As demonstrated in the inset of Fig. 11, the triazole-functionalized MCLs remained unaffected by the introduction of Pb^{2+} ions but did deflect in response to the introduction

of Hg^{+2} ions. In order to make comparisons with other experiments, the result shown in the insert was divided into two parts. The first part shows the response of the MCLs to the injection of distilled water and the Pb^{2+} solution and is represented by the purple curves at the top of Fig. 11. The second part representing the deflection resulting from the introduction of Hg^{2+} ions is also shown in purple and is labelled as $Hg(ClO_4)_2$ proceeded by $Pb(ClO_4)_2$. This data was shifted in time so that the injection of the $Hg(ClO_4)_2$ coincided with the initial injection of the $Pb(ClO_4)_2$ solution. The results reveal that the sensitivity of triazole-functionalized MCLs towards Hg^{2+} was altered, leading to a decrease of approximately 44 % in the microcantilever deflection compared to the case where Hg^{2+} ions were injected immediately after water (black curves in Fig. 11). In order to gain more insight into the reaction mechanism of the triazole-functionalized MCLs, a solution containing equal concentrations of Hg^{2+} and Pb^{2+} was presented to the triazole-functionalized MCLs. As shown by the blue curves in Fig. 11, the microcantilever deflection decreased by approximately 52% compared to the deflection produced by the sequential injection of Pb^{2+} and Hg^{2+} (i.e. purple curves) and by 87% to the deflection produced by Hg^{2+} alone (i.e. black curves). An additional experiment was conducted this time using a solution having a concentration of 10^{-5} M solution with Pb^{2+} being 25% of the Hg^{2+}. As shown by the red curves in Fig. 11, the microcantilever deflection increased compared to the deflection produced by the equal amounts of Hg^{2+} and Pb^{2+}. By calculating the end deflection at 35 min for the deflection curves shown in Fig.11, we can infer that approximately 85% of the triazole functional layer reacted with Hg. From these results we can infer that the Pb^{2+} ion are in fact interacting

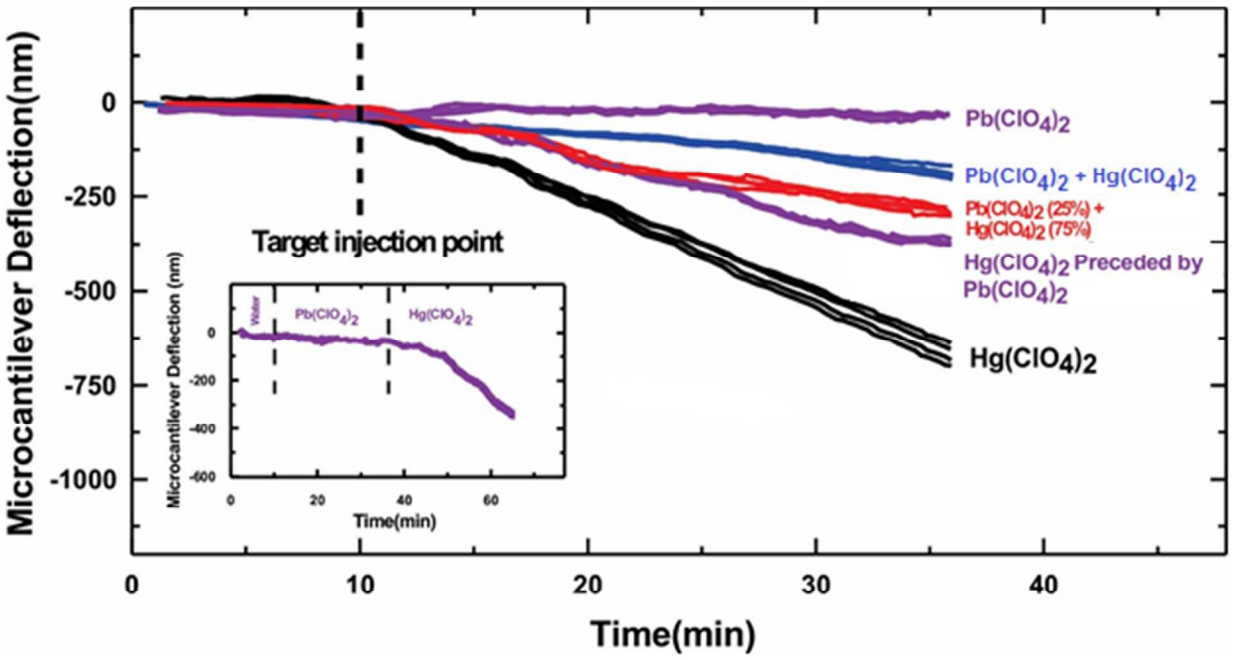

Fig. 11. The influence of the presence of $Pb(ClO_4)_2$ to the sensitivity of triazole-functionalized MCLs towards $Hg(ClO_4)_2$. The inset shows the deflection produced as a result of a sequential introduction of Pb^{+2} and Hg^{+2}.

3. Computational study

We have previously reported density-functional theory (DFT) computational studies to complement the experimentally observed binding studies.[22-24] These DFT studies have also supported the assignment of the likely coordination sites in imidazolyl- and pyridyl-functionalized ionophoric thiacalix[4]arenes.

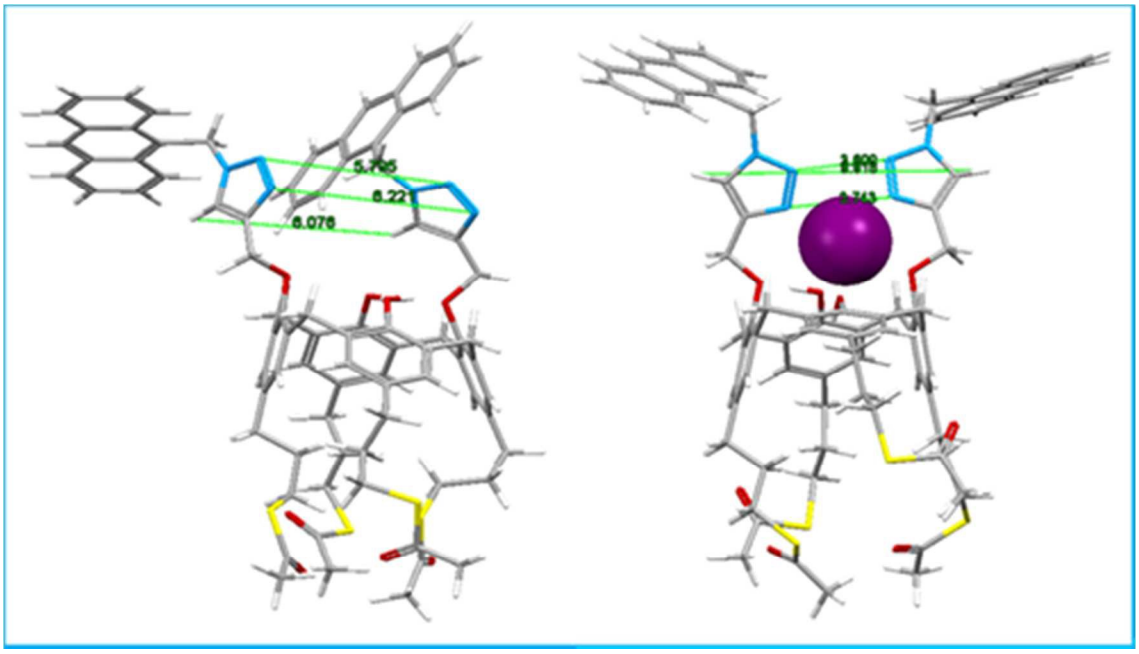

Fig. 12. Geometry-optimized (PBE0/LANL2DZ) structures of **2** and as its Hg^{2+}complex. *Left*: The free host **2**; *right*: 1:1 **2**⊃Hg^{2+} complex. Colour code: carbon = dark grey; oxygen = red, nitrogen = blue, sulphur = yellow and Hg^{2+} = purple.

In the present study, the geometries of the molecular structures were optimized with either the B3LYP or PBE0 functionals with the LANL2DZ basis set. The DFT level of theory using the hybrid Perdew-Burke-Ernzerhof parameter free-exchange correlation functional PBE0 (PBE1PBE in the Gaussian realization)[25] with the Hay and Wadt effective core potential LANL2DZ basis set.[26] The starting structure was generated using SpartanPro'10 with the MMFF94 method.[27] The generated structures were then imported into *Gaussian-09*[28] and were geometry-optimized in the gas-phase with the PBE0 functional with the LANL2DZ basis set. Lower energies (i.e. more energetically-favoured structures) were obtained using the PBE0 functionals and these are the ones which are compared and described below. The N--N distance between the triazole ring nitrogens decreases from 5.795 Å to 3.609 Å and 6.221 Å to 3.743 (Å) since the nitrogen atoms moved inwards after complexing **2** with Hg^{2+} (as shown in Fig. 12). The H--H distance between the triazolyl ring hydrogen atoms increases from 6.079 Å to 9.918 Å, as

the hydrogen atoms are moved outwards. Since the ^{1}H NMR titration complex study shows that the triazolyl ring hydrogen signals are shifted downfield by +0.91 ppm after complexation with Hg^{2+}, this is in agreement with the computational result for the H--H distance change noted, from 6.076 Å to 9.918 Å.

The binding or interaction energies (IE) using the PBE0/LANL2DZ basis set were calculated according to the following equation: $IE = E_{Complex} - \Sigma(E_{Calixtriazole} + E_M{}^{n+})$:where M^{n+} = Pb^{2+}, Hg^{2+} or Fe^{3+}. Thus, for [**2** + Pb^{2+} – 2H)] IE values were computed to be: –1426.8 kJ/mole for the binding of the Pb^{2+} in the lower rim i.e. between the two triazole moieties, compared with only –1226.7 kJ/mole for binding of the Pb^{2+} in the wide- or upper-rim where the thioacetate groups are situated. For the [**2** + (Hg^{2+} – $2H^+$)] complex the corresponding IEs values were –1130.0 kJ/mole and –806.kJ/ mol, respectively. For the [**2** + (Fe^{3+} – $2H^+$)]$^+$ complex the corresponding IEs were –3637.8 kJ/mole and –3441.3 kJ/mol, respectively.

In all three cases examined there was a more energetically favoured gas-phase complex formed with the individual ions in the lower rim than with those in the upper rim. On the basis of the magnitudes of the computational data obtained, is interesting that the Pb^{2+} complex appears to be more favoured than that of the corresponding Hg^{2+} complex. Although the Fe^{3+} complex appeared to have the lowest energy, it must be noted that this complex would still have a positive charge so presumably should not be directly compared with the others.

4. Experimental section

Complexation studies were conducted using UV-vis and fluorescence spectroscopy. UV-vis spectra were recorded on an Agilent 8543 Diode Array spectrophotometer connected to an HP computer. Emission spectra were measured on a Photon Technology

International (PTI) Quanta Master 6000 spectrofluorometer equipped with a continuous xenon arc lamp as the excitation source. The emitting light was collected at 90° to the excitation beam and was detected by a Hammamatsu R-928 photomultiplier tube (PMT) in the photon counting mode. All emission spectra were corrected for instrumental light loss using correction factors supplied by PTI. All of the metal ion salts as their perchlorates were purchased from Alfa Aesar in >99 % purity. High-purity spectral grade $CHCl_3$ and CH_3CN were purchased from Cambridge Isotope Laboratories.

4.1 Preparation of the microcantilever sensor arrays

MCL sensor arrays used in this work (CLA500-010-08l, Concentris, GmbH, Switzerland), were approximately 500-μm in length, 100-μm wide and 1-μm thick. All experiments performed during this work were conducted using two 8-microcantilever arrays. Cantilevers functionalized with the calixarene sensing layer will be referred to as the active cantilevers whereas reference cantilevers are those coated with a SAM of decanethiol. Both active and reference cantilevers were subjected to identical cleaning and thin film deposition conditions. The complete removal of organic residue, oxide layer, and ionic contaminants was accomplished by treating the MCL arrays with the RCA cleaning method.[29] MCL arrays were then dried in an oven at 275° C for 5 min. Following the cleaning process, the MCL arrays were coated with 5 nm of Inconel (0.8 Ni:0.2 Cr) followed by 40-nm of gold by sputter deposition. The use of Inconel ensures sufficient adhesion of the gold film onto the silicon cantilevers. The formation of the SAM of **2** onto the Au surface was conducted by immersing the MCLs in a 1:9 dichloromethane:ethanol solution of **2** (2.0×10^{-5} M) for 2 h (active arrays). The preparation of the reference cantilevers was performed by incubating them for 2 h in a 1.0

μM solution of decanethiol. The incubation of each cantilever was performed using a home-made functionalization unit that allows each cantilever to be functionalized individually. The final cantilever deflection measurements were obtained by subtracting the deflection of the reference cantilever to the deflection of the active cantilever, to obtain a differential signal providing a measure of the mcirocantilever deflection caused only by the interaction between calixarene sensing layer and the target ions.

4.2 Microcantilever experimental setup

MCL sensing measurements were carried out in an experimental system capable of holding two 8-microcantilever arrays fabricated in our laboratories. A detailed discussion of the development of this system is as yet unpublished. In brief, following the functionalization of the cantilever arrays with the proper sensing layers, the arrays were transferred and sealed into a flow-through cell. Research-grade distilled water was first introduced at a flow rate of 0.1 ml/min until thermal equilibrium was achieved. Arrays were then exposed to a constant flow of aqueous solutions containing the target ions. The response of MCLs during the molecular interactions was monitored using an optical beam deflection system where a laser beam reflected from the MCLs was directed into a 2-D position-sensitive detector (PSD). The PSD output was then used to obtain the MCL deflection.

Conclusions

A new bimodal calix[4]arene which is functionalized in the narrow-rim 1,3-positions with triazolyl-linked anthhracenyl groups and in all four of the wide-rim positions with 3-propyl-thioacetate groups has been synthesized. This new calix[4]arene formed an effective SAM on Au in a multi-arrayed microcantilever instrument and was shown to be

a sensitive and reproducible receptor for low concentrations of Hg^{2+} in aqueous solutions. The cantilever sensor data showed excellent reproducibility between each cantilever varying by approximately ±5% of the deflection signal. Based on the obtained data it should be possible to measure concentrations as low as 10^{-13} with our existing system. Binding studies in solution by fluorescence titration and competitive studies confirmed this Hg^{2+} sensitivity. DFT computational studies were in agreement with the likely site of binding of the metal as suggested by a ^{1}H-NMR study. Finally, the results presented herein clearly reveal the high sensitivity of triazole-functionalized microcantilevers by responding differently to the injection of different concentrations of Hg^{2+}. We have also shown that triazole-functionalized microcantilevers showed the highest sensitivity towards Hg^{2+} ions over the other metal ions which were tested. The mass spectral data indicated that more than a single Hg^{2+} could bind to the receptor molecule in solution where the thioacetate groups are not immobilized onto the Au layer of the MCLs.

Acknowledgements

We thank the research support from the Research Development Corporation, Vale, Memorial University of Newfoundland and the Ministry of Higher Education, Kingdom of Saudi Arabia for the Scholarship to MB and ANA. The computational work has been assisted by the use of computing resources provided and by WestGrid and Compute/Calcul Canada and assisted by Dr. G. Shamov.

Notes and references

[a]Department of Physics and Physical Oceanography, Memorial University of Newfoundland, St. John's, Newfoundland and Labrador, Canada A1B3X7. E-mail: lbeaulieu@mun.ca; Fax: +1 709 864 8739; Tel: +1 709 864 6203.

[b]Department of Chemistry, Memorial University of Newfoundland, St. John's, Newfoundland and Labrador, Canada A1B3X7. E-mail: parisg@mun.ca; Fax: +1 709 864 3702; Tel: +1 709 864 8517.

† Electronic Supplementary Information (ESI) available: ^{1}H-, ^{13}C-NMR and MS data for compounds **2** and **4**.

1- (a) P. E. Georghiou, S. Rahman, G. Valluru, L. N. Dawe, A. N. Alodhayb and L. Y. Beaulieu, *New J. Chem.,* 2013*,* **37**, 122-1301. (b) G. Valluru, S. Rahman, P. E. Georghiou, L. N. Dawe, A. N. Alodhayb and L. Y. Beaulieu, *New J. Chem.,* 2014*,* **38**, 5868-5872. (c) A. Alodhayb, S. M. S Rahman, S. Rahman, G. K. Valluru, P. E. Georghiou and L. Y. Beaulieu, *Sens. Actuators B,* 2014, **203**, 766-773.

2- (a) C. D. Gutsche, *Calixarenes: An Introduction: Edition 2*. Royal Society of Chemistry, 2008. (b) *Calixarenes 2001*, Z. Asfari, V. Böhmer, J. Harrowfield and J. Vicens, J., Eds.: Kluwer Academic, Dordrecht, The Netherlands, 2001. (c) L. Mandolini and R. Ungaro, Eds, *Calixarenes in Action,* Imperial College Press, London, 2000.

3- (a) B. Mokhtari, K. Pourabdollah, and N. Dalali, *J. Coord. Chem*. 2011, **64**, 743-794. (b) V. Arora, H. M. Chawla, and S. P. Singh, A*rkivoc*, **2007***, 2*, 172-200.

4- H. J. Kim, M. H. Lee, L. Mutihac, J. Vicens, J. and J. S. Kim, *Chem. Soc. Rev.* 2012, **41**, 1173-1190; *and references cited therein*.

5- (a) H.-F. Ji, E. Finot, R. Dabestani, T. Thundat, G. M. Brown and P. F. Britt, *Chem. Commun*., 2000, 457–458. (b) H. Chen, Y.-S. Gal, S.-H. Kim, H.-J. Choi,M.-C. Oh, J. Lee and K. Koh, *Sens. Actuators, B*, 2008, **113**, 577–581.

6- P. S. Waggoner and H. G. Craighead, *Lab Chip*, 2007, **7**, 1238-1255.

7- N. V. Lavrik, M. J. Sepaniak and P. G. Datskos, *Rev. Sci. Instrum.* 2004, **75**, 2229-2253.

8- J. K. Gimzewski, C. Gerber, E. Meyer and R, R. Schlittler, *Chem. Phys. Lett.*, 1994, **217**, 589-594.

9- M. Álvarez, L. G. Carrascosa, M. Moreno, A. Calle, Á. Zaballos, L. M. Lechuga and J. Tamayo, *Langmuir*, 2004, **20**, 9663-9668.

10- R. Datar, S. Kim, S. Jeon, P. Hesketh, S. Manalis, A. Boisen and T. Thundat, *MRS Bulletin*, 2009, **34**, 449-454.

11- A. Alodhayb, N. Brown, S. M. S. Rahman, R. Harrigan and L. Y. Beaulieu, *Appl. Phys. Lett*, 2013, **102**, 173106.

12- L. Y. Beaulieu, M. Godin, O. Laroche, V. Tabard-Cossa and P. Grütter, *Ultramicroscopy*, 2007, **107**, 422-430.

13- J. O. Duruibe, M. O. C. Ogwuegbu and J. N. Egwurugwu, J. N. *Int. J Phys. Sci.* 2007, **2**, 112-118.

14- V. V. S. Mummidivarapu, V. K. Hinge, K. Tabbasum, R. G. Gonnade, and C. P. Rao, *J. Org. Chem.* **2013**, *78*, 3570-3576.

15- (a) K.-C. Chang, I.-H. Su, A. Senthilvelan and W.-S. Chung, *Org. Lett.* 2007, **9**, 3363-3366. (b) K.-C. Chang, I.-H. Su, G.-H. Lee and W.-S. Chung, *Tetrahedron Lett*. 2007, **48**, 7274-7278. (c) N.-J. Wang, C.-M. Sun and W.-S. Chung, *Sens. Actuators B*, 2012, **171– 172**, 984–993 (d) R. K. Pathak, V. K. Hinge, K. Mahesh, A. Rai, D. Panda and C. P. Rao, *Anal. Chem.* 2012, **84**, 6907-6913. (e) J. Cho, T. Pradhan, J. S. Kim and, S. Kim, *Org. Lett.* 2013, **15**, 4058-4061.

16- (a) P. Thordarson, *Chem. Soc. Rev.* 2011, **40**, 1305-1323. (b) **http://supramolecular.org**

17- (a) A. Ojida, Y. Mito-oka, M.-A. Inoue and I. Hamachi, *J. Am. Chem. Soc.* 2002, **124**, 6256-6258. (b) M. Choi, M. Kim, K. D. Lee, K.-N. Han, I.-A. Yoon, H.-J. Chung and J. Yoon, *Org. Lett.* 2001, **3**, 3455-3457. (c) M.-Y. Chae, X. M. Cherian and A. W. Czarnik, *J. Org. Chem.* 1993, **58**, 5797-5801.

18- Y-J. Chen, S.-C. Yang, C.-C. Tsai, K.-C. Chang, W.-H. Chuang, W.-L. Chu, V. Kovalev and W.-S. Chung, *Chem. Asian. J.* 2015, **10**, 1025-1034.

19- (a) J. J. Lee, S. A. Lee, H. Kim, L-T. Nguyen, I. Noh and C. Kim, *RSC Adv*. 2015, **4**, 41905-41913; (b) Y. Ma, F. Wang, S. Kambam and X. Chen, *Sens. Actuators B*, 2013, **188**, 1116-1122; (c) A. Gogoi, S. Samanta and G. Das , *Sens. Actuators B*, 2014, **202**, 788-794; (d), X-l. Ni, Y. Wu, C. Redshaw and T. Yamato, *Dalton Trans*. 2014, **43**, 12633-12638; (e) N. C. Lim, J. V. Schuster, M. C. Porto, M. A. Tanudra, L. Yao, H. C. Freake, and C. Brückner, *Inorg. Chem*., 2005, **44**, 2018-2030.

20- S.-S. Li, L.-P. Xu, L.-J. Wan, S.-T. Wang, L. Jiang, *J. Phys. Chem B.* 2006, **110**,1794

21- X. Xu, T. G., Thundat, G. M. Brown and H. F. Ji, *Anal. Chem.*, 2002, **74**, 3611-3615.

22- J.-L. Zhao, H. Tomiyasu, X.-L. Ni, X. Zeng, M. R. J. Elsegood, C. Redshaw, S. Rahman, P. E. Georghiou and T. Yamato, *New J. Chem.* 2014, **38**, 6041-6049.

23- J.-L. Zhao, H. Tomiyasu, X.-L. Ni, X. Zeng, M. R. J. Elsegood, C. Redshaw, S. Rahman, P. E. Georghiou, S. J. Teat and T. Yamato, *Org. Biomol. Chem.* 2015, **13**, 3476-3483.

24- S. Rahman, Y. Assiri, A. N. Alodhayb, L. Y. Beaulieu, A. Oraby, P. E. Georghiou, *New J. Chem.,* 2016, DOI: 10.1039/C5NJ01362C.

25- (a) J. P. Perdew, K. Burke and M. Ernzerhof, *Phys. Rev. Lett.*, 1996, **77**, 3865-3868; (b) J. P. Perdew, K. Burke and M. Ernzerhof, *Phys. Rev. Lett.,* 1997, **78**, 1396.

26- (a) P. J. Hay and W. R. Wadt, *J. Chem. Phys.*, 1985, **82**, 270; (b) P. J. Hay and W. R. Wadt, *J. Chem. Phys.*, 1985, **82**, 284; (c) P. J. Hay and W. R. Wadt, *J. Chem. Phys.*, 1985, **82**, 299.

27- Initial molecular modeling calculations using the MMFF94 were performed using the PC *Spartan'10* software from Wavefunction Inc., Irvine, CA.

28- M. J. Frisch, G. W. Trucks, H. B. Schlegel, G. E. Scuseria, M. A. Robb, J. R. Cheeseman, G. Scalmani, V. Barone, B. Mennucci, G. A. Petersson, H. Nakatsuji, M. Caricato, X. Li, H. P. Hratchian, A. F. Izmaylov, J. Bloino, G. Zheng, J. L. Sonnenberg, M. Hada, M. Ehara, K. Toyota, R. Fukuda, J. Hasegawa, M. Ishida, T. Nakajima, Y. Honda, O. Kitao, H. Nakai, T. Vreven, Jr. J. A. Montgomery, J. E. Peralta, F. Ogliaro, M. Bearpark, J. J. Heyd, E. Brothers, K. N. Kudin, V. N. Staroverov, T. Keith, R. Kobayashi, J. Normand, K. Raghavachari, A. Rendell, J. C. Burant, S. S. Iyengar, J. Tomasi, M. Cossi, N. Rega, J. M. Millam, M. Klene, J. E. Knox, J. B. Cross, V. Bakken, C. Adamo, J. Jaramillo, R. Gomperts, R. E. Stratmann, O. Yazyev, A. J. Austin, R. Cammi, C. Pomelli, J. W. Ochterski, R. L. Martin, K. Morokuma, V. G. Zakrzewski, G. A. Voth, P. Salvador, J. J. Dannenberg, S. Dapprich, A. D. Daniels, O. Farkas, J. B. Foresman, J. V. Ortiz, J. Cioslowski and D. J. Fox, *Gaussian 09, Revision D.01*; Gaussian, Inc., Wallingford CT, 2013.

29- W. Kern, *Handbook of semiconductor wafer cleaning technology*. 111-196, Noyes Publications, Park Ridge, New Jersey, 1993.

Metal ion binding properties of a bimodal triazolyl-functionalized calix[4]arene on a multi-array microcantilever system. Synthesis, fluorescence and DFT computation studies.

Abdullah N. Alodhayb,[a] Mona Braim,[a] L.Y. Beaulieu[a], Gopikishore Valluru,[b] Shofiur Rahman,[b] Ahmed K. Oraby [b] and Paris E. Georghiou [b*]